

# Anomalous couplings in the $t\bar{t}+Z$ final state at the HL-LHC

Lukas Lechner, Daniel Spitzbart, Robert Schöfbeck

## 1 Introduction

Many beyond the Standard Model (BSM) predictions include anomalous couplings of the top quark to the electroweak gauge bosons [1–7]. While we restrict this study to the  $t\bar{t}Z$  channel and the CMS Phase-2 detector with a luminosity scenario of  $3\text{ ab}^{-1}$ , we go beyond earlier work [8] and study the sensitivity of the  $t\bar{t}Z$  process using differential cross section data. We interpret the result in terms of the SM effective field theory [9] and set limits on the relevant Wilson coefficients of the Warsaw basis [10]  $C_{tZ}$ ,  $C_{tZ}^{[Im]}$ ,  $C_{\phi t}$  and  $C_{\phi Q}$  [11, 12].

## 2 Event simulation

We generate events at the parton level at LO using **MADGRAPH5aMC@NLO** v2.3.3 [13], and decay them using **MadSpin** [14, 15]. Parton showering and hadronization are done using **PYTHIA** 8.2 [16, 17]. Fast detector simulation was performed using **Delphes** [18], with the CMS reconstruction efficiency parametrization for the Phase-2 upgrade. The mean number of interactions per bunch crossing (pileup, PU) is varied from 0 to 200. Jets are reconstructed with the FastJet package [19] and using the anti- $k_T$  algorithm [20] with a cone size  $R = 0.4$ . Besides the signals, we also generate the main backgrounds in the leptonic final states in order to achieve a realistic background prediction. The  $WZ$ ,  $tZq$ ,  $tWZ$ ,  $t\bar{t}\gamma$  and  $t\bar{t}Z$  processes are normalized to cross sections calculated up to next-to-leading order (NLO) in perturbative QCD.

## 3 Event selection

From results on the inclusive  $t\bar{t}Z$  cross section from ATLAS [21, 22] and CMS [23–26] it follows that the three lepton channel, where the  $Z$  and one of the  $W$  bosons originating from a top quark decay leptonically is the most sensitive search channel. We thus require three reconstructed leptons ( $e$  or  $\mu$ ) with  $p_T(l)$  thresholds of 10, 20, and 40 GeV, respectively, and  $|\eta(l)| < 3.0$ . We furthermore require that there is among them a pair of opposite-sign same-flavor leptons consistent with the  $Z$  boson by requiring  $|m(l\bar{l}) - m_Z| < 10\text{ GeV}$ . We remove reconstructed leptons within a cone of  $\Delta R < 0.3$  to any reconstructed jet satisfying  $p_T(j) > 30\text{ GeV}$ . Furthermore, at least 3 jets are required with  $p_T(j) > 30\text{ GeV}$  and  $|\eta(j)| < 4.0$ , where one of the jets has been identified as a  $b$ -tag jet according to the **Delphes** specification.

We consider the distributions of the observables above in equally sized bins of the transverse  $Z$  boson momenta  $p_T(Z)$  [27] and  $\cos\theta_Z^*$ , the relative angle of the negatively charged lepton to the  $Z$  boson direction of flight in the rest frame of the boson. The differential cross sections for the SM (black) and BSM (colored lines) interpretations in  $t\bar{t}Z$  with respect to  $p_T(Z)$  and  $\cos\theta_Z^*$  are shown in Fig. 1

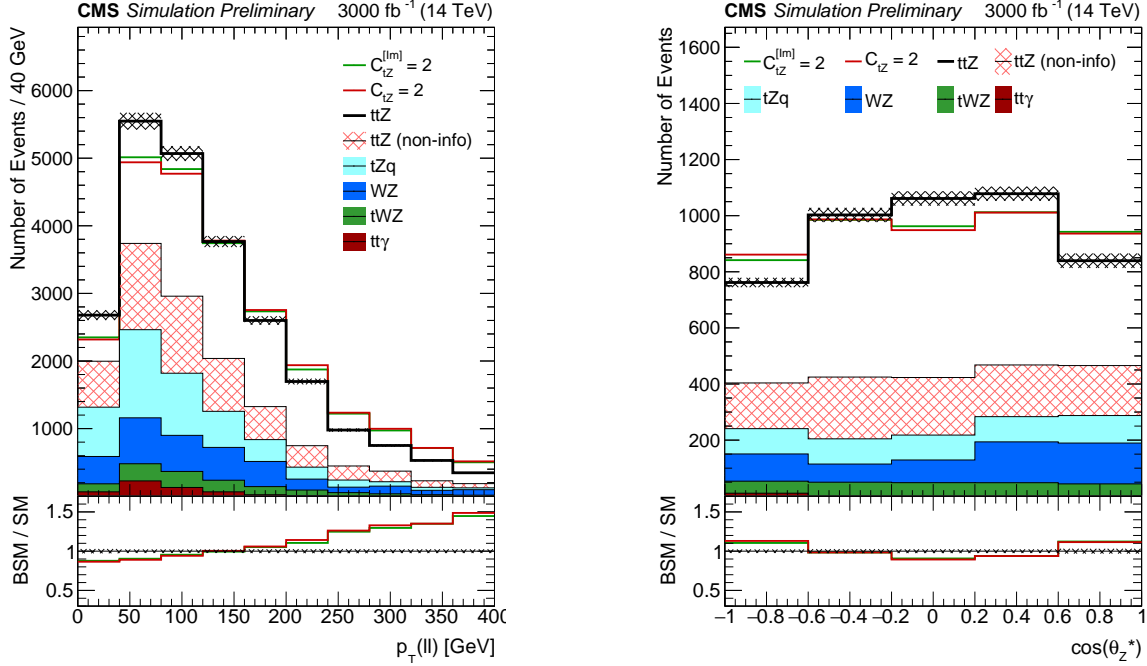


Figure 1: Differential cross sections of  $p_T(Z)$  (left) and  $\cos \theta_Z^*$  (right) for the in the text mentioned selection and the Phase-2 scenario. For  $\cos \theta_Z^*$ , additionally  $p_T(Z) > 200$  GeV is applied.

for  $C_{tZ} = 2 (\Lambda/\text{TeV})^2$  and  $C_{tZ}^{[Im]} = 2 (\Lambda/\text{TeV})^2$ . We normalize the BSM distributions to the SM yield in the plots to visualize the discriminating features of the parameters. The part of the signal which does not contain information on the Wilson coefficients is shown hatched, backgrounds are shown in solid colors.

## 4 Results

The predicted yields are estimated for the  $3 \text{ ab}^{-1}$  HL-LHC scenario at  $\sqrt{s} = 13$  TeV and scaled to 14 TeV, where an additional small background from non-prompt leptons is taken from Ref. [26] and scaled to  $3 \text{ ab}^{-1}$ . We perform a profiled maximum likelihood fit of the binned likelihood function  $L(\theta)$  and consider  $q(r) = -2 \log(L(\hat{\theta})/L(\hat{\theta}_{\text{SM}}))$ , where  $\hat{\theta}$  and  $\hat{\theta}_{\text{SM}}$  are the set of nuisance parameters maximizing  $L(\theta)$  at the BSM and SM point, respectively. Experimental uncertainties are estimated based on the expected performance of the Phase-2 CMS detector. In Fig. 2, the likelihood scan for the  $t\bar{t}Z$  process is shown, where one Wilson coefficients at a time is considered non-zero. The corresponding 68% and 95% CL intervals are summarized in Table 2. In Fig. 3 we consider two pairs of Wilson coefficients corresponding to modified neutral current interactions ( $C_{\phi t}$  and  $C_{\phi Q}$ ), and dipole moment interactions ( $C_{tZ}$  and  $C_{tZ}^{[Im]}$ ). The Wilson coefficient not shown on the  $x$  axis is included in the profiling of nuisance parameters. The corresponding 68% and 95% CL intervals are summarized in Table 1. In Fig. 4, the log-likelihood scan for the  $t\bar{t}Z$  process is shown in the  $C_{\phi Q}/C_{\phi t}$  parameter plane (left) and the dipole moment parameter plane  $C_{tZ}/C_{tZ}^{[Im]}$  (right). The green (red) lines show the  $1\sigma$  ( $2\sigma$ ) contour line and the SM parameter point corresponds to  $C_{\phi t} = C_{\phi Q} = 0$  and  $C_{tZ} = C_{tZ}^{[Im]} = 0$ .

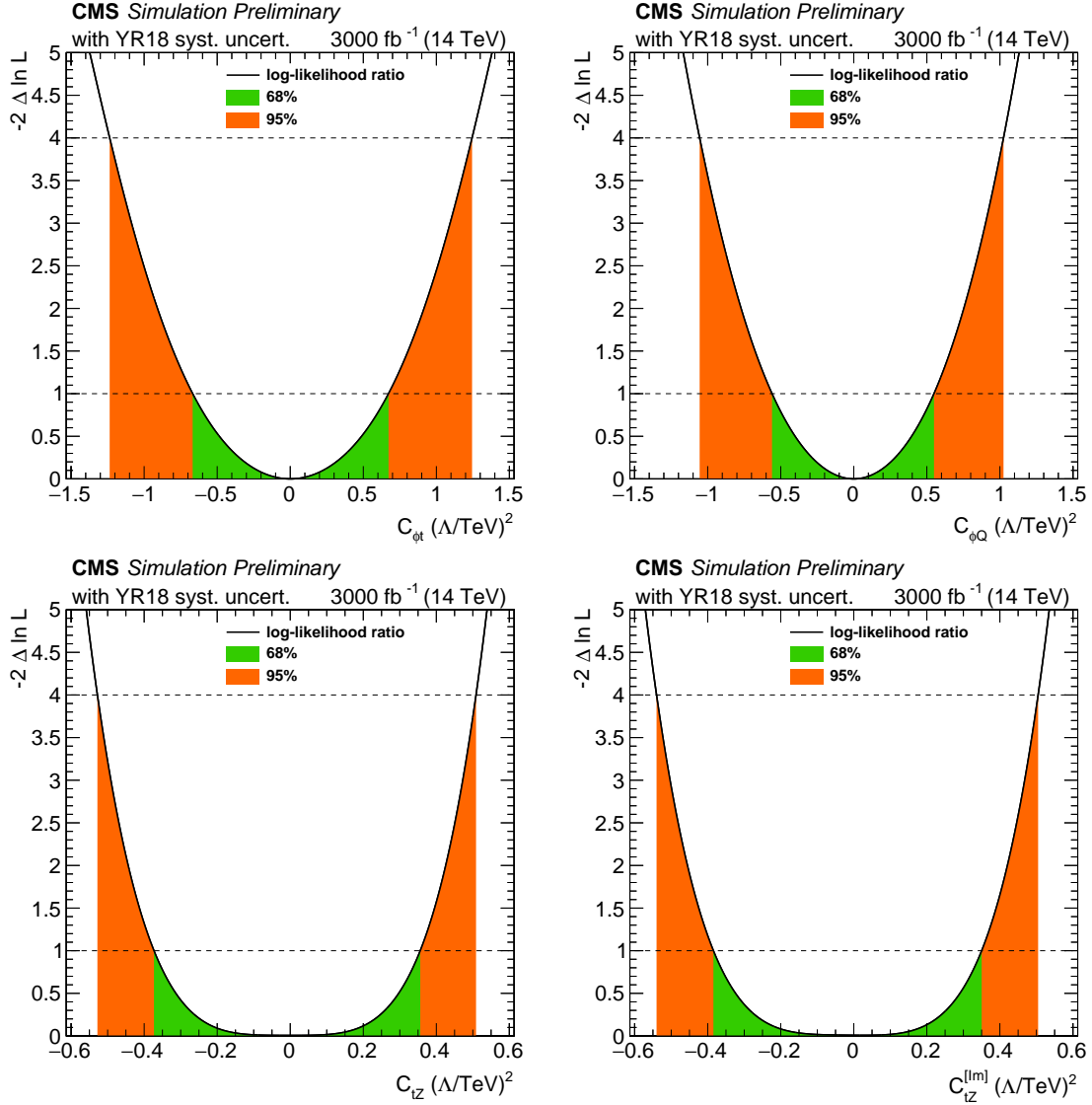


Figure 2: Individual likelihood ratio for the Wilson coefficients  $c_{pt}$  and  $c_{pQM}$  (top) and  $c_{tZ}$  and  $c_{tZI}$  (bottom) for the  $ttZ$  process. Here, only one Wilson coefficient at a time is considered non-zero. The  $\pm 1\sigma$  ( $\pm 2\sigma$ ) intervals are given in green (red).

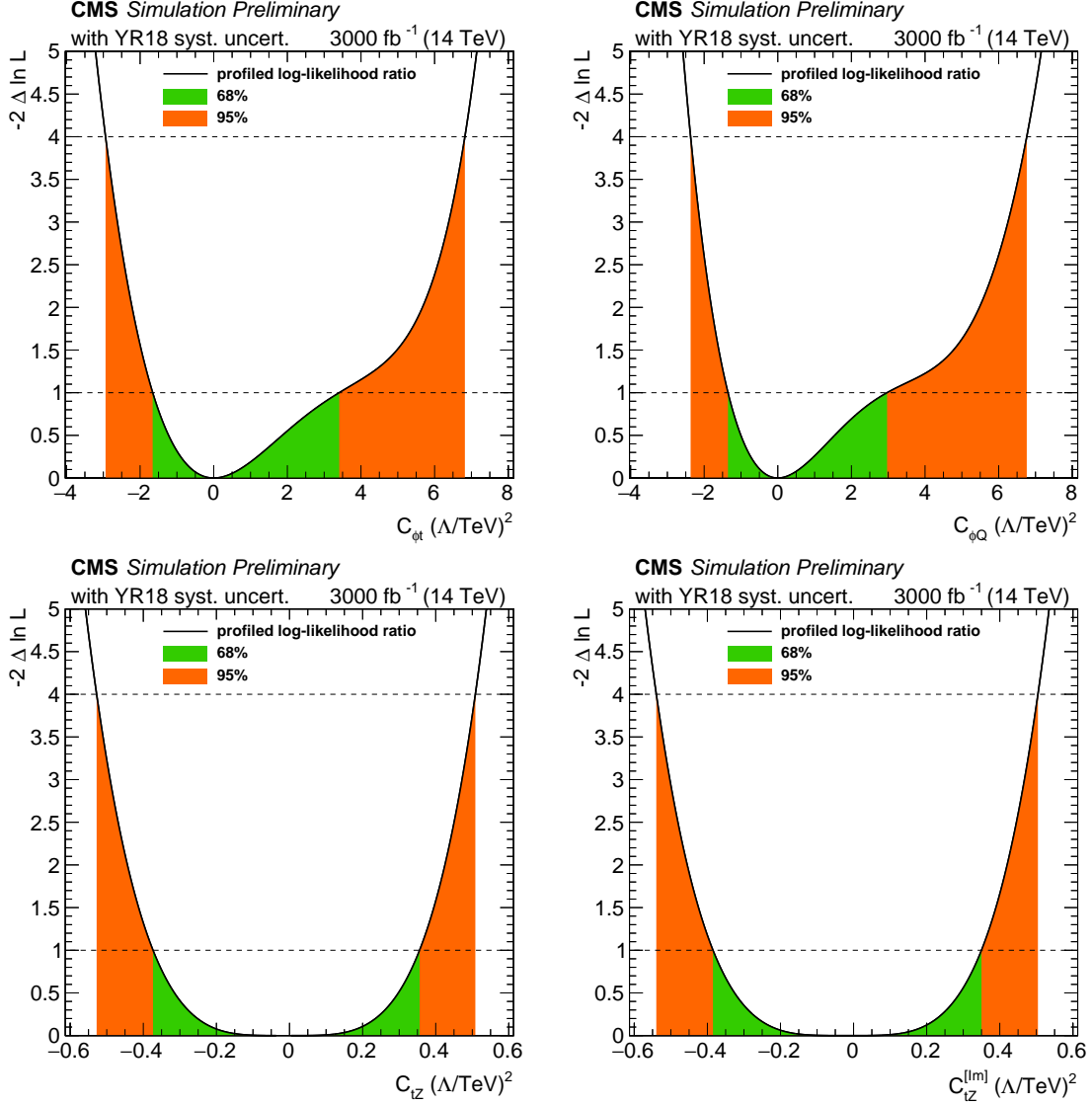


Figure 3: Individual profiled likelihood ratio for the Wilson coefficients  $C_{\phi t}$  and  $C_{\phi Q}$  (top) and  $C_{tZ}$  and  $C_{tZ}^{[Im]}$  (bottom) for the  $t\bar{t}Z$  process under the SM hypothesis. The  $\pm 1\sigma$  ( $\pm 2\sigma$ ) intervals are given in green (red).

Table 1: Expected 68 % and 95 % CL intervals for the selected Wilson coefficients in a profiled scan.

Wilson coefficient	68 % CL $(\Lambda/\text{TeV})^2$	95 % CL $(\Lambda/\text{TeV})^2$
$C_{\phi t}$	[-1.66, 3.41]	[-2.94, 6.82]
$C_{\phi Q}$	[-1.35, 2.97]	[-2.37, 6.76]
$C_{tZ}$	[-0.37, 0.35]	[-0.53, 0.51]
$C_{tZ}^{[\text{Im}]}$	[-0.38, 0.35]	[-0.54, 0.50]

Table 2: Expected 68 % and 95 % CL intervals, where one Wilson coefficient at a time is considered non-zero.

Wilson coefficient	68 % CL $(\Lambda/\text{TeV})^2$	95 % CL $(\Lambda/\text{TeV})^2$
$C_{\phi t}$	[-0.67, 0.67]	[-1.24, 1.24]
$C_{\phi Q}$	[-0.56, 0.55]	[-1.05, 1.02]
$C_{tZ}$	[-0.37, 0.35]	[-0.53, 0.51]
$C_{tZ}^{[\text{Im}]}$	[-0.38, 0.35]	[-0.54, 0.50]

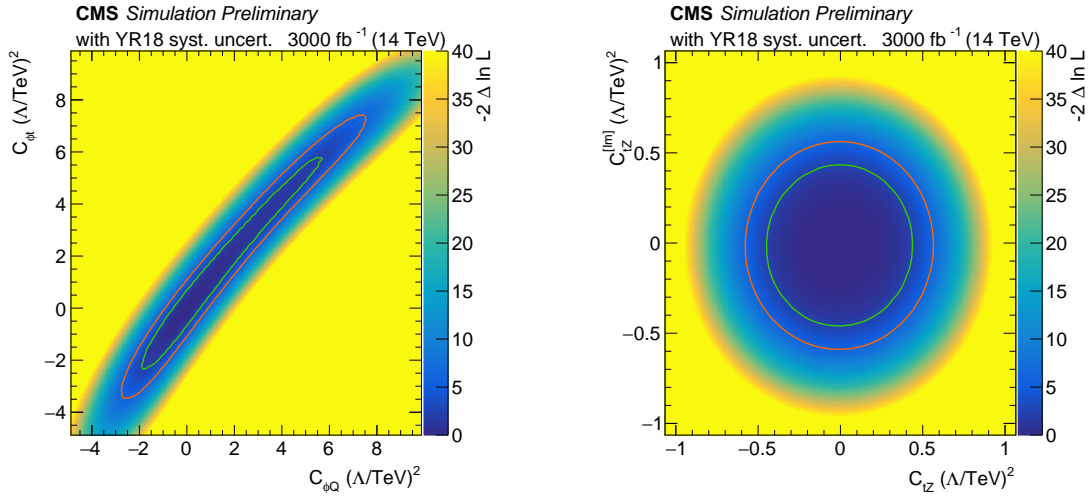


Figure 4: Scan of the negative log-likelihood in the  $C_{\phi Q}/C_{\phi t}$  (left) and  $C_{tZ}/C_{tZ}^{[\text{Im}]}$  parameter planes (right) for the  $t\bar{t}Z$  process. The  $\pm 1\sigma$  ( $\pm 2\sigma$ ) contour lines are given in green (red).

## References

- [1] W. Hollik, Jose I. Illana, S. Rigolin, C. Schappacher, and D. Stockinger. Top dipole form-factors and loop induced CP violation in supersymmetry. *Nucl. Phys.*, B551:3, 1999. [Erratum: Nucl. Phys.B557,407(1999)].
- [2] Kaustubh Agashe, Gilad Perez, and Amarjit Soni. Collider Signals of Top Quark Flavor Violation from a Warped Extra Dimension. *Phys. Rev.*, D75:015002, 2007.
- [3] Alexander L. Kagan, Gilad Perez, Tomer Volansky, and Jure Zupan. General Minimal Flavor Violation. *Phys. Rev.*, D80:076002, 2009.
- [4] Tarek Ibrahim and Pran Nath. The Top quark electric dipole moment in an MSSM extension with vector like multiplets. *Phys. Rev.*, D82:055001, 2010.
- [5] Tarek Ibrahim and Pran Nath. The Chromoelectric Dipole Moment of the Top Quark in Models with Vector Like Multiplets. *Phys. Rev.*, D84:015003, 2011.
- [6] Christophe Grojean, Oleksii Matsedonskyi, and Giuliano Panico. Light top partners and precision physics. *JHEP*, 10:160, 2013.
- [7] François Richard. Can LHC observe an anomaly in  $t\bar{t}Z$  production? 2013.
- [8] Raoul Roentsch and Markus Schulze. Probing top-Z dipole moments at the LHC and ILC. *JHEP*, 08:044, 2015.
- [9] D. Barducci et al. Interpreting top-quark LHC measurements in the standard-model effective field theory. 2018.
- [10] B. Grzadkowski, M. Iskrzynski, M. Misiak, and J. Rosiek. Dimension-Six Terms in the Standard Model Lagrangian. *JHEP*, 10:085, 2010.
- [11] Johann Brehmer, Kyle Cranmer, Felix Kling, and Tilman Plehn. Better Higgs boson measurements through information geometry. *Phys. Rev.*, D95(7):073002, 2017.
- [12] Johann Brehmer. *New Ideas for Effective Higgs Measurements*. PhD thesis, U. Heidelberg (main), 2017.
- [13] J. Alwall, R. Frederix, S. Frixione, V. Hirschi, F. Maltoni, O. Mattelaer, H. S. Shao, T. Stelzer, P. Torrielli, and M. Zaro. The automated computation of tree-level and next-to-leading order differential cross sections, and their matching to parton shower simulations. *JHEP*, 07:079, 2014.
- [14] Pierre Artoisenet, Rikkert Frederix, Olivier Mattelaer, and Robbert Rietkerk. Automatic spin-entangled decays of heavy resonances in Monte Carlo simulations. *JHEP*, 03:015, 2013.
- [15] Stefano Frixione, Eric Laenen, Patrick Motylinski, and Bryan R. Webber. Angular correlations of lepton pairs from vector boson and top quark decays in Monte Carlo simulations. *JHEP*, 04:081, 2007.
- [16] Torbjorn Sjöstrand, Stephen Mrenna, and Peter Z. Skands. A brief introduction to PYTHIA 8.1. *Comput. Phys. Commun.*, 178:852, 2008.

- [17] Torbjörn Sjöstrand, Stefan Ask, Jesper R. Christiansen, Richard Corke, Nishita Desai, Philip Ilten, Stephen Mrenna, Stefan Prestel, Christine O. Rasmussen, and Peter Z. Skands. An introduction to PYTHIA 8.2. *Comput. Phys. Commun.*, 191:159, 2015.
- [18] J. de Favereau, C. Delaere, P. Demin, A. Giammanco, V. Lemaître, A. Mertens, and M. Selvaggi. DELPHES 3, A modular framework for fast simulation of a generic collider experiment. *JHEP*, 02:057, 2014.
- [19] Matteo Cacciari, Gavin P. Salam, and Gregory Soyez. FastJet User Manual. *Eur.Phys.J.*, C72:1896, 2012.
- [20] Matteo Cacciari, Gavin P. Salam, and Gregory Soyez. The Anti-k(t) jet clustering algorithm. *JHEP*, 0804:063, 2008.
- [21] Georges Aad et al. Measurement of the  $t\bar{t}W$  and  $t\bar{t}Z$  production cross sections in pp collisions at  $\sqrt{s} = 8$  TeV with the ATLAS detector. *JHEP*, 11:172, 2015.
- [22] ATLAS Collaboration. Measurement of the  $t\bar{t}Z$  and  $t\bar{t}W$  production cross sections in multi-lepton final states using  $3.2 \text{ fb}^{-1}$  of pp collisions at  $\sqrt{s} = 13$  TeV with the ATLAS detector. *Eur. Phys. J. C*, 77:40, 2017.
- [23] Serguei Chatrchyan et al. Measurement of associated production of vector bosons and  $t\bar{t}$  in pp collisions at  $\sqrt{s} = 7\text{TeV}$ . *Phys. Rev. Lett.*, 110:172002, 2013.
- [24] Vardan Khachatryan et al. Measurement of top quark-antiquark pair production in association with a W or Z boson in pp collisions at  $\sqrt{s} = 8$  TeV. *Eur. Phys. J. C*, 74:3060, 2014.
- [25] Vardan Khachatryan et al. Observation of top quark pairs produced in association with a vector boson in pp collisions at  $\sqrt{s} = 8$  TeV. *JHEP*, 01:096, 2016.
- [26] Albert M Sirunyan et al. Measurement of the cross section for top quark pair production in association with a W or Z boson in proton-proton collisions at  $\sqrt{s} = 13$  TeV. *JHEP*, 08:011, 2018.
- [27] Raoul Roentsch and Markus Schulze. Constraining couplings of top quarks to the Z boson in  $t\bar{t} + Z$  production at the LHC. *JHEP*, 07:091, 2014. [Erratum: JHEP09,132(2015)].